Direct surface charging and alkali-metal doping for tuning the interlayer magnetic order in planar nanostructures

Tamene R. Dasa* and Valeri S. Stepanyuk†
Max-Planck-Institut für Mikrostrukturphysik, Weinberg 2, D-06120 Halle, Germany
(Received 27 February 2015; published 10 August 2015)

The continuous reduction of magnetic units to ultrasmall length scales inspires efforts to look for a suitable means of controlling magnetic states. In this study, we show two surface charge alteration techniques for tuning the interlayer exchange coupling of ferromagnetic layers separated by paramagnetic spacers. Our *ab initio* study reveals that already a modest amount of extra charge can switch the mutual alignment of the magnetization from antiferromagnetic to ferromagnetic or vice versa. We also propose adsorption of alkali metals as an alternative way of varying the electronic and chemical properties of magnetic surfaces. Clear evidence is found that the interlayer magnetic order can be reversed by adsorbing alkali metals on the magnetic layer. Moreover, alkali-metal overlayers strongly enhance the perpendicular magnetic anisotropy in FePt thin films. These findings combined with atomistic spin model calculations suggest that the electronic or ionic way of surface charging can have a crucial role for magnetic hardening and spin state control.

DOI: 10.1103/PhysRevB.92.075412 PACS number(s): 73.22.−f, 75.30.Gw, 75.70.−i, 75.10.Hk

I. INTRODUCTION

In the field of spin electronics, there have been efforts made in recent years to discover efficient ways to manipulate memory units and logic devices [1,2] as well as to minimize their size. In the past few decades, the reading scheme of the modern hard disk drive was reduced to the nanoscale level following the discovery of the giant magnetoresistance effect in metallic multilayers by Grunberg and Fert [3,4]. Current technology uses tunneling magnetoresistance to read the state of magnetic units [5,6]. It relies on the relative alignment of the magnetic layers interspaced by the coupling medium, which results in the difference of the tunneling resistance. The existence of such intriguing characteristics is related to the delocalized electrons within the coupling medium that are confined. Apart from the advancement in the reading mechanism of the state of the magnetic units, the writing head still makes use of a magnetic field that is less able to control magnetic states on short length scales. Alternatively, such magnetic states can be reversed using the current-induced spin-transfer torque technique in which the spin-polarized current tunnels through the junction, consequently producing spin torque [7,8]. It has also been shown that the mutual magnetization in the magnetic tunneling junction can be tuned by applying a voltage, and this effect has a similar order of magnitude to that of spin-transfer torque [9–11].

Recently, both density-functional theory [12–16] and experimental studies [1,17,18] have revealed a more efficient method, on the basis of magnetoelectric coupling, for tuning the spin alignment in a ferromagnet (FM).

For instance, the anisotropy properties of a two-dimensional (2D) ferromagnet could be tuned by varying its intrinsic charge carriers [12,15] or the oxidation state using electric means [19]. On the other hand, an external electric field was used in combination with multiferroic materials to reverse the relative alignment of ferromagnets separated by a nonmagnetic medium (FM/NM/FM) [20–22]. Theoretical studies have shown that the interlayer exchange coupling and magnetoresistance effect are interrelated [23,24]. Nonetheless, direct manipulation of the interlayer exchange coupling is one of the most feasible and perhaps least investigated approaches for a tuning magnetic order. It would even be more compelling to find a possible way to tune magnetic coupling or anisotropy in planar nanostructures with ionic doping.

Our study verifies a possible route for manipulating the interlayer exchange coupling (IEC) and the relative alignment of the magnetic layers interspaced by nonmagnetic multilayers, employing direct surface charging and alkali-metal adsorption. The former mechanism relies on sequential variation of the intrinsic charge concentration of the FM/NM/FM multilayer, and the results related to this phenomenon are presented in Sec. III. Additionally, in Sec. IV we propose that the process of surface charge alteration can be accomplished by adsorbing free-electron systems, i.e., alkali metals, on surfaces. Indeed, this mechanism alters the electrochemical features of the magnetic surface and leads to a reversal of the relative spin alignment. Apart from tuning the interlayer magnetic order, the magnetic anisotropy of the Fe/Pt multilayer can be significantly enhanced using alkali-metal deposition. To better appreciate such an increase of the magnetic anisotropy energy, in Sec. V the hysteresis loop for the FePt multilayer is plotted through the atomistic spin model approach. A discussion and analysis of these findings is presented in Sec. VI, followed by our conclusion in Sec. VII.

II. COMPUTATIONAL DETAILS

A thorough *ab initio* study was performed within the projector augmented wave technique (PAW) [25] as implemented in the VASP code [26,27]. The local spin density approximation (LSDA) is used for the exchange and correlation interactions [28]. A plane-wave basis set is used to describe the Kohn-Sham wave function, and in all calculations a plane-wave cutoff energy of 430 eV was used. A dense k-point mesh of $21 \times 21 \times 1$ and a smearing width of 2 meV, which

*trdasa@mpi-halle.de
†stepanyu@mpi-halle.de

were tested for their reliability, were employed to obtain a more accurate value of the magnetic anisotropy energy (MAE) and the IEC. We have used a supercell approach in which two layers of Fe separated with a finite number of Cu spacers are supported by a Pt(001) substrate [29]. The surface charging effect is introduced by sequentially varying the number of valence electrons. Additionally, a uniform charge background is assumed [30]. Doping of alkali metals is done by capping the top magnetic layer with two different structures of Na or Li overlayers, namely $p(1 \times 1)$ and $c(2 \times 2)$. For the latter configuration, a 2×2 supercell is used. The pairwise exchange coupling or simply the interlayer exchange coupling (E_{IEC}) was calculated as $E_{\mathrm{IEC}} = E_{\mathrm{AF}} - E_{\mathrm{FM}}$, and for all charge states the spins were aligned along their easy axes. For the 2×2 supercell, the interlayer coupling is calculated as $E_{\mathrm{IEC}} = \frac{1}{4}(E_{\mathrm{AF}} - E_{\mathrm{FM}})$. To determine the easy axis of magnetization, we have performed a fully relativistic calculation including spin-orbit coupling [31]. The MAE is evaluated by taking the energy difference between two axes of magnetization, i.e., parallel ([100]) and perpendicular ([001]) to the surface plane. A similar procedure is followed to calculate the MAE for an antiferromagnetic configuration, and the two spins are oriented antiparallel to each other for both axes of magnetization. Hereafter, we shall denote the charge added to the multilayers (net charge) as $q_{+(-)}$, whereas n stands for the charge density of the entire system.

To study the magnetization reversal in FePt planar nanostructures, we use the atomistic spin model approach [32]. This phenomenon can be investigated by mapping the magnetic properties already investigated on the basis of electronic structure theory with atomistic spin models. In the latter case, the energetics of interacting spin with an effective magnetic moment is described by a spin Hamiltonian, which has the form

$$\mathbf{H} = \sum_{i \neq j} J_{ij}\mathbf{S}_i \cdot \mathbf{S}_j - k_u \sum_i (\mathbf{S}_i \cdot \mathbf{e})^2 - \sum_i \mu_s \mathbf{S}_i \cdot \mathbf{H}_{\mathrm{app}}, \tag{1}$$

where the first, middle, and last terms describe the exchange interaction (H_{exc}), magnetic anisotropy (H_{MAE}), and the external magnetic field (H_{app}) or Zeeman term, respectively. J_{ij} denotes the exchange coupling parameters between atomic sites i and j, and the local spin moments are denoted with unit vectors $\mathbf{S}_i$ and $\mathbf{S}_j$ obtained from the realistic atomic moments as $\mathbf{S}_i = m_s/|m_s|$. The exchange coupling parameters and the single-ion anisotropy in Eq. (1) are obtained from calculations on the basis of density-functional theory. The magnetization curves are simulated by solving the stochastic Landau-Lifshitz-Gilbert (LLG) equation. At the atomic level, the LLG equation is written as

$$\frac{\partial \mathbf{S}_i}{\partial t} = -\frac{\gamma}{(1+\lambda^2)}\mathbf{S}_i \times [\mathbf{H}_{i,\mathrm{eff}} + \lambda(\mathbf{S}_i \times \mathbf{H}_{i,\mathrm{eff}})], \tag{2}$$

where $\gamma = 1.76 \times 10^{11}\ \mathrm{T}^{-1}\,\mathrm{s}^{-1}$ is the absolute value of the gyromagnetic ratio, λ is the damping parameter, and the atomistic effective magnetic field is denoted by $\mathbf{H}_{i,\mathrm{eff}}$. The effective magnetic field is derived from the spin Hamiltonian shown in Eq. (1) [32]. The FePt multilayers are modeled with two Fe layers separated with an effective medium that extends as 6 nm $\times$ 7 nm within the xy plane. When simulating the magnetization curve, the thermal effect and the magnetostatic field are taken into consideration and are included in the effective magnetic field [32,33]. Further discussion on the hysteresis loop of FePt multilayers is presented in Sec. V.

III. SWITCHING INTERLAYER EXCHANGE COUPLING WITH SURFACE CHARGING

First, we present the results concerned with the influence of direct surface charging on the relative magnetization of two magnetic layers separated with a Cu spacer. When the charge neutrality of metallic multilayers is perturbed by additional positive or negative charges, it leads to spatial charge redistribution mainly toward the surface. A reduced variation of the spatial charge is also observed underneath the surface.

Such charge redistribution can even be spin-dependent, which can alter the magnetic order [13,15]. Meanwhile, the exchange interaction across the coupling medium in the Fe/$\mathrm{Cu_N}$/Fe trilayer, supported on a Pt(001) substrate, determines the magnetic state to be either ferromagnetic (FM) or antiferromagnetic (AF). For such multilayers, we demonstrate a strong effect of direct surface charging on the relative magnetic order. As an illustration, in Fig. 1 the variation of the interlayer exchange coupling for Fe/$\mathrm{Cu_N}$/Fe multilayers in response to the addition or removal of charges is depicted for a Cu spacer thickness of $N = 4$ and 7 layers. The Fe layers separated with four layers of Cu (uncharged) are coupled antiferromagnetically, and the E_{IEC} is found to be -2.5 meV. The antiferromagnetic coupling can be further enhanced by

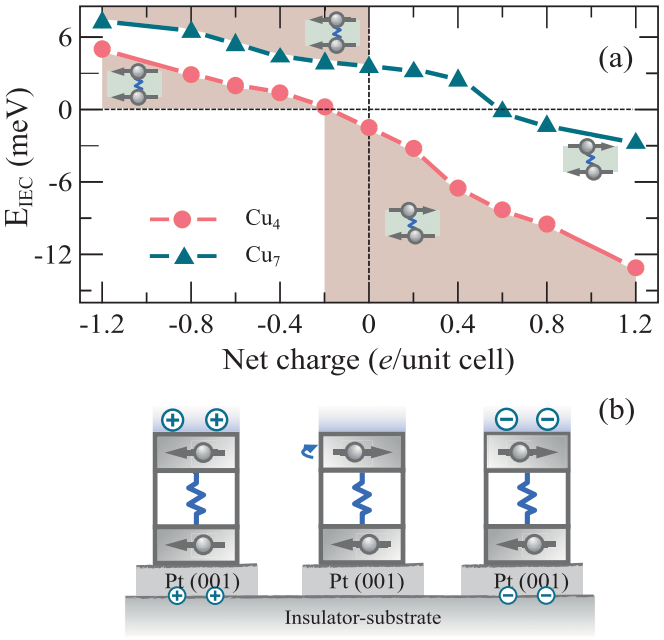

FIG. 1. (Color online) (a) The interlayer exchange coupling (IEC) between the magnetic layers in Fe/$\mathrm{Cu_N}$/Fe multilayers on Pt(001) as a function of the net charge in the system. As an illustration, such relations are plotted for a Cu spacer thickness of $N = 4$ (circle) and $N = 7$ (triangle). (b) A schematic description of Fe/$\mathrm{Cu_4}$/Fe and the relative alignment of the magnetization as a result of charge injection or removal.

negative charge doping. As an example, by injecting negative charge of the order of $\Delta q = 1.2\ \bar{e}$ per unit cell [34] in $Fe/Cu_4/Fe$, the absolute value of the E_{IEC} is increased to 12 meV. The most fascinating finding is observed when the electron concentration is reduced from the neutral $Fe/Cu_4/Fe$, which results in the switching of the relative magnetic order from antiferromagnetic to ferromagnetic coupling. Explicitly, switching from an AF to a FM configuration takes place when the system is charged with 0.2 h per unit cell, and a further increment of the extra holes to 1.2 h per unit cell leads to an E_{IEC} of ∼5 meV.

An essential issue now could be the interplay of the finite-size effect, i.e., the thickness of the Cu spacer, surface charging, and interlayer exchange coupling. To study this phenomenon, exchange coupling (E_{IEC}) with respect to charge injection is investigated for thicker Cu layers. In Fig. 1(a), we have employed seven layers of Cu as a mediator in which the IEC of the uncharged system is 3.6 meV. Similar to the case of four layers, here space-charge variation has a significant effect on the IEC. The addition of a certain amount of negative charges switches the magnetic coupling to AF. Interestingly, for $Fe/Cu_7/Fe$ multilayers a transition of the easy axis of magnetization from the in-plane to the out-of-plane direction and the reversal of the relative magnetic order are observed at the same charge state, i.e., at 0.6 $\bar{e}$/unit cell. In another multilayer, i.e., the $Fe/Cu_6/Fe$ trilayer, we found that the magnetic moments are counteraligned for all charge states. However, the influence of negative charge injection on the IEC is much stronger than the positive ones. In other words, the absolute value of the IEC for the neutral system (∼6 meV) is reduced by 75% as soon as the system is injected with 1 $\bar{e}$ per unit cell. One should note that for the experimental realization of effective surface-interface charging, the alloy multilayers should be electrically decoupled by a semiconductor or an insulator, as shown in Fig. 1(b), and hence the net charge is trapped in the upper layers.

IV. ALKALI-METAL-INDUCED SWITCHING OF THE INTERLAYER MAGNETIC ORDER

So far we have shown the impact of charge injection on magnetic order by controlling the intrinsic charge carriers. Nevertheless, controlling the number of charge carriers in a slab could be an experimentally challenging task. Therefore, efforts are underway to find an alternative method of varying the surface electronic structure. Recently it was shown that incorporating a net charge in a nanostructure can be achieved by an electrolyte [35–37] or by adding dopants [38], while using a scanning tunneling microscope or an electron force microscope tip is also an indispensable option [39]. Doping of magnetic entities with alkali metals or halogens can lead to a significant variation of their electrochemical properties [40,41] as well as their spin properties [42,43]. Moreover, alkali metals are illustrative free-electron systems, and they have relatively small ionization energies. Here we verify that alkali metals deposited on a magnetic surface can be employed as a natural way of varying the electronic and chemical properties of FM/NM/FM trilayers, and the magnetic properties could be controlled as well. In particular, the interplay between the deposition of alkali metals and the change in the interlayer

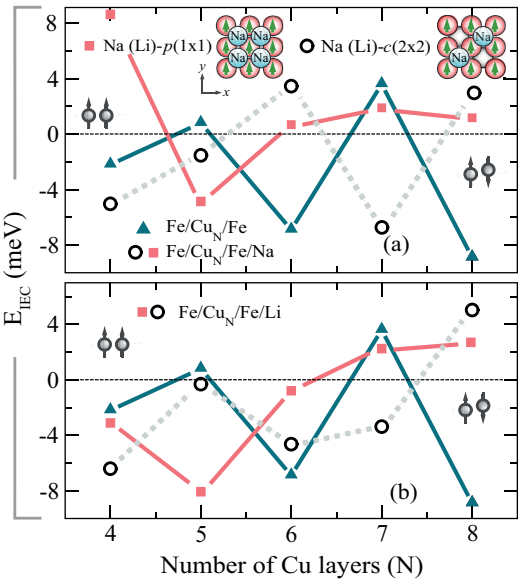

FIG. 2. (Color online) (a) Impact of Na adsorption on the IEC in $Fe/Cu_N/Fe$ (triangles) and $Fe/Cu_N/Fe/Na$-$p(1 \times 1)$ (squares) for different thickness of Cu spacer. The values of the IEC for the $c(2 \times 2)$ configuration of Na (top) on the magnetic layer are represented with circles. The inset shows the $p(1 \times 1)$ and $c(2 \times 2)$ structures of Na or Li adsorbates on the magnetic surface. (b) Similar plot on the variation of the IEC for $Fe/Cu_N/Fe$ and $Fe/Cu_N/Fe/Li$ (rectangles and circles) multilayers with respect to Cu spacer thickness. The IEC of the $Fe/Cu_N/Fe/Li$ multilayer with a $p(1 \times 1)$ (rectangles) and a $c(2 \times 2)$ (circles) configuration of the Li capping layer is also presented.

magnetic coupling is investigated. In Fig. 2(a), the values of the IEC for $Fe/Cu_N/Fe$ and $Na/Fe/Cu_N/Fe$ multilayers are presented. The magnetic coupling of $Fe/Cu_N/Fe$ oscillates between FM and AF order as the thickness of the spacer increases, which is related to the quantum-well states (QWSs) in the Cu multilayers [23,44]. In fact, the results for six, seven, and eight Cu layers of the neutral systems are compared with available studies based on the Korringa-Kohn-Rostoker method [45], and the magnetic order as well as the exchange coupling energies are in very good agreement.

We have considered two structures of Na (Li) on the Fe surface, namely Na (Li)-$p(1 \times 1)$ and Na (Li)-$c(2 \times 2)$ structures, in order to gain more insight into the influence of the Na (Li) coverage on the IEC. The former and latter adsorbate structures cover the magnetic surface fully and partially, respectively. The configuration of these two structures on the magnetic surface is shown in Fig. 2(a) (see the inset). The Na ions are adsorbed at the hollow site, which was identified as the most favorable one for alkali-metal adsorbates [40,46]. Regarding the magnetic coupling, adsorption of Na ions on the magnetic surface brought about an intriguing change to the interlayer exchange coupling. As shown in Fig. 2(a) (square), when the Fe layer is fully covered with Na [$p(1 \times 1)$], all the magnetic states of $Fe/Cu_N/Fe$ are switched from FM to AF or from AF to FM, except for $N = 7$. In particular, a strong change on the IEC, accompanied by magnetic reversal, is observed when the Cu spacer thicknesses are four and eight layers. Reducing the Na layer coverage by half, from

Na-$p(1 \times 1)$ to Na-$c(2 \times 2)$, can also lead to a significant change in the IEC. As shown in Fig. 2(a) (circles), capping the $Fe/Cu_N/Fe$ multilayer with Na-$c(2 \times 2)$ changes the magnetic order from FM (for the uncapped multilayers) to AF when the spacer thicknesses are five and seven Cu layers ($N = 5$ and 7). Moreover, the same configuration of Na varies the interlayer magnetic coupling in the $Fe/Cu_{6,8}/Fe$ multilayer from AF to FM. However, covering the top Fe layer of $Fe/Cu_4/Fe$ with submonolayer Na-$c(2 \times 2)$ does not switch the magnetic order. Switching the relative magnetic order can be accomplished by increasing the Na coverage, suggesting that the IEC depends on the percentage of coverage of the Na overlayer. An additional manifestation of the effect of Na coverage on the IEC can be seen on the $Fe/Cu_7/Fe$ trilayer. In this multilayer when the Na coverage is reduced by 50%, from $p(1 \times 1)$ to $c(2 \times 2)$, the IEC changes from 2 meV (FM order) to -7 meV (AF order), respectively. These observations led us to the conclusion that variations of the IEC induced by Na depends on the configuration of the adsorbate (percentage coverage) as well as on the spacer thickness.

Similar investigations have been done by using Li ions as a dopant instead of Na [squares in Fig. 2(b)]. Covering the $Fe/Cu_N/Fe$ structures with a single layer of Li-$p(1 \times 1)$ tends to reduce the value of IEC for $N = 7$ and increases the absolute value of the IEC for antiferromagnetically coupled $Fe/Cu_4/Fe$. Moreover, the magnetic order is reversed from FM ($Fe/Cu_5/Fe$) to AF ($Fe/Cu_5/Fe/Li$) when the spacer thickness is five Cu layers. Conversely, for $Fe/Cu_{6,8}/Fe$ trilayers, Li doping has a tendency to reduce the strength of AF coupling, and even the relative magnetic order in $Fe/Cu_8/Fe$ is changed to FM coupling (for $Fe/Cu_8/Fe/Li$) as result of Li doping. In Fig. 2(b), we have also presented the IEC for the $Fe/Cu_N/Fe/Li - c(2 \times 2)$ multilayer, shown as circles. Reducing the percentage coverage of Li ions from $p(1 \times 1)$ to $c(2 \times 2)$ here can only change the strength of the exchange coupling. Only for the case of $Fe/Cu_7/Fe/Li$-$p(1 \times 1)$ can the mutual magnetic order be switch to AF coupling by reducing the Li coverage [Li-$c(2 \times 2)$] of the magnetic surface. Interestingly, the changes in the IEC of FeCu multilayers that are caused by a $p(1 \times 1)$ configuration of both Na and Li ions are the same. Moreover, FeCu multilayers that are doped with Na-$c(2 \times 2)$ and Li-$c(2 \times 2)$ also show similar exchange coupling in most cases. All in all, except in a few cases, the trends by which Li or Na ions change the IEC are analogous to one another, implying that a similar tuning of the relative magnetization in FM/NM/FM multilayers can also be accomplished by other alkali metals.

V. MAGNETIC HARDENING OF FePt MULTILAYERS WITH Na IONS

We have demonstrated a remarkable effect of direct surface charging and alkali-metal doping on interlayer exchange coupling. It is also worthwhile to investigate the impact of Na ions on the MAE, which determines the stability of magnetic systems. In this regard, materials with FePt composition are known to have high MAE [14,47,48] and are used for current high-density recording media [49]. Here, we show that the MAE of the FePt multilayer can be further enhanced by adsorption of Na ions. To verify this magnetic hardening effect,

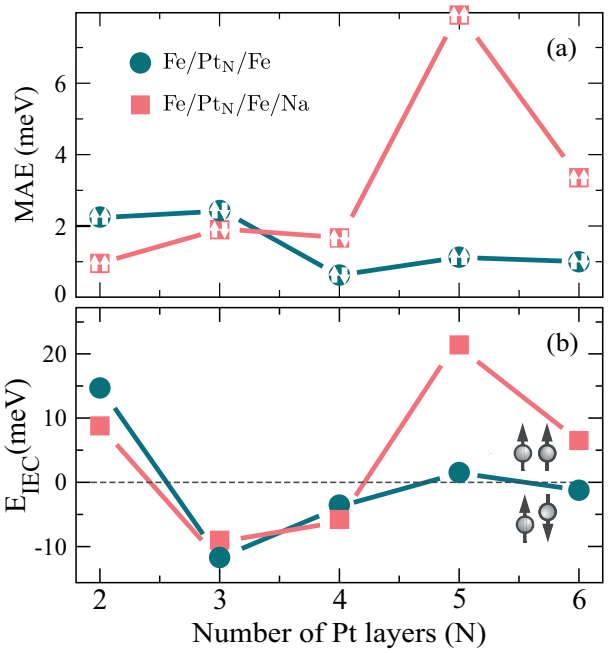

FIG. 3. (Color online) (a) The MAE of the stable magnetic orders in $Fe/Pt_N/Fe$ (circle) and $Na/Fe/Pt_N/Fe$ (square) for different thickness of Pt spacer. The arrows in the square and circle indicate the respective magnetic order for which the magnetic anisotropy is evaluated. (b) The corresponding plot for the interlayer exchange coupling where positive and negative values of the IEC represent ferromagnetic and antiferromagnetic couplings, respectively.

we consider a model system that consists of two Fe layers separated with Pt multilayers, and these $Fe/Pt_N/Fe$ stacks are supported by a Pt(001) substrate. We calculate the MAE as the difference in energy between two axes of magnetization of the system, i.e., $MAE = E_x - E_z$. An identical calculation is carried out for the Fe/Pt_N bilayer on Pt(001) in order to estimate the layer-resolved MAE and its relation with the interlayer magnetic coupling [58].

In Fig. 3(a), the MAE of the $Fe/Pt_N/Fe$ trilayer is plotted as a function of the Pt spacer thickness, with (squares) and without (circles) the adsorption of Na ions. The values of the MAE are presented for the stable magnetic configurations, and in all cases the easy axis of magnetization is aligned perpendicular to the surface. The FePt multilayers with smaller spacer thicknesses ($N = 2,3$) show high values of MAE relative to the thicker ones. A decrease in the value of the MAE of $Fe/Pt_N/Fe$ is observed when the Pt spacer thickness increases from $N = 3$ to 4. A further increment of the spacer thickness brings about a small change to the magnetic anisotropy, and an average MAE of 1 meV is observed. As shown in Fig. 3(b) (circles), for $Fe/Pt_{2,5}/Fe$ the stable magnetic order is found to be ferromagnetic, whereas antiferromagnetic coupling is observed for $N = 3$, 4, and 6. Indeed, the interlayer magnetic order for $Fe/Pt_2/Fe$ is in agreement with other similar systems [50]. Additionally, experimental and theoretical studies have verified the existence of such variation of the interlayer exchange coupling between FM and AF coupling in similar systems [51,52].

Basically, Pt is very close to the Stoner criterion and can be magnetized when it hybridizes with a ferromagnet. For example, we found that the nearest Pt layer has a magnetic moment up to $0.35\mu_B$ in Fe/Pt_N/Fe multilayers. In such systems, the competition of the induced magnetization from the upper and lower Fe layers determines the magnetic configuration in the neighboring Pt layers, more importantly for $N \leqslant 3$, and probably the magnetic order within the multilayer. As a consequence of such competition, the Fe/$Pt_{2,3}$/Fe trilayers could be driven away from Stoner instability, leading to antiferromagnetic order. Certainly, the effect of the spin-polarized QWS on the IEC still exists, especially for FePt multilayers with a thicker Pt spacer. Even more, such magnetic coupling can be affected by the Na capping layer. For instance, a strong change of the IEC is depicted for Fe/$Pt_{5,6}$/Fe, in Fig. 3(b), by Na adsorption, whereas the Na capping layer induces a moderate change for other FePt multilayers. An additional perspective on the tuning of the IEC in relation to the MAE and Na overlayer is pointed out in the latter part of Sec. VI.

As already mentioned in the earlier sections, one of the main goals of this study is to point out the impact of alkali-metal deposition on the magnetic anisotropy of FePt thin films. In Fig. 3(a), contrary to the uncapped multilayers, the FePt multilayers that are capped with a Na monolayer show high MAE for thicker spacer thicknesses. Clearly, one can see that Na adsorption strongly enhances the MAE when the Pt spacer thicknesses are four, five, and six atomic layers. As an example, deposition of Na ions on Fe/Pt_6/Fe trilayers (AF coupling) significantly enhances the MAE from ∼1 to ∼3.4 meV, increasing the energy barrier more than threefold. Exceptionally, for the system whereby the two Fe layers are interspaced with five Pt layers, Na ion capping increases the MAE to ∼8 meV. Moreover, we have compared the change in the MAE and the IEC, and it is clearly seen that the systems with the strongest IEC correspond to the highest MAE. Specifically, we have already shown that Na deposition strongly increases the IEC of Fe/Pt_5/Fe trilayers from 1.5 to 22 meV. The next higher change in the IEC induced by the Na overlayer is observed when spacer thicknesses of four and six Pt layers are employed. Likewise, the change in the MAE is relatively large. These results clearly suggest that the enhancement of the MAE is almost directly related with the absolute value of the change in the interlayer exchange coupling. Moreover, they verify that the magnetic order and anisotropy of such complex alloy magnetic systems could be altered as a result of ionic doping, leading to a change in the magnetic stability and dynamics [55,56]. It is an experimentally proven fact that the magnetic order of such FM/NM/FM trilayers remains unchanged for thicker ferromagnetic layers [53,54], which explains the interplay between magnetic order and anisotropy.

TABLE I. The exchange parameters (J_1, J_2, and J_3 [meV/$(\mu_B)^2$]), spin magnetic moments m_s[Fe_1(Fe_2)](μ_B), and the estimated MAE (in meV) of two Fe layers interspaced with five layers of Pt.

	J_1	J_2	J_3	MAE_1	MAE_2	m_s[Fe_1(Fe_2)]
$Fe_2/Pt_5/Fe_1$	5.1	4.9	0.2	0.1	1.2	[2.9 (2.7)]
$Fe_2/Pt_5/Fe_1$/Na	4.7	4.9	1.4	1.6	6.3	[2.7 (2.9)]

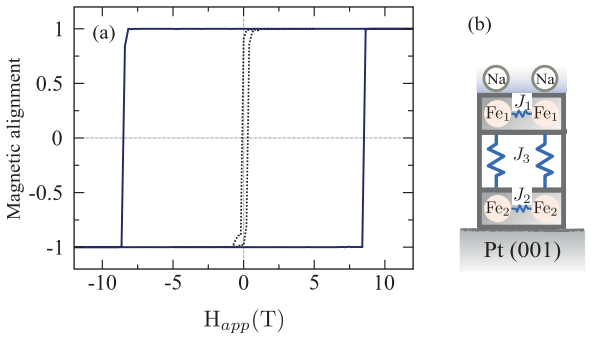

FIG. 4. (Color online) (a) The hysteresis loop of Fe/Pt_5/Fe trilayers with (full lines) and without (dotted lines) Na capping layers. The simulations are performed for the out-of-plane direction, which is the easy axis of magnetization. (b) An illustrative diagram of the exchange coupling parameters within the multilayer.

Apart from the magnetic properties discussed above, the magnetization reversal process is studied by simulating the hysteresis loop for FePt multilayers. To do this, we apply an external magnetic field within the range of −12 to 12 T. The calculation is performed within the stochastic Landau-Lifshitz-Gilbert (LLG) equation. The LLG equation [Eq. (2)] is integrated by using the Heun integration scheme [57], with a time step of $\triangle t = 1$ fs. The simulation temperature is set to be 5 K, and the damping parameter $\lambda = 1.0$ is used for the sake of computational efficiency. The values of the exchange coupling parameters, J_1, J_2, and J_3, as well as the estimated values of the MAE are presented in Table I [58]. We have created a model system of two Fe layers separated with an effective spacer. Figure 4 illustrates the hysteresis loops for both FePt multilayers with (full lines) and without (dotted lines) Na deposition. Both multilayers show squarelike hysteresis loops. One can see that the Na capping layer significantly increases the coercive field to $H_a = \sim 8.5$ T. Therefore, the atomistic spin model simulations clearly demonstrate that alkali-metal doping of FePt multilayers favors domain nucleation at elevated temperature by increasing the energy barrier. Furthermore, it indicates that the magnetic hardening effect can be accomplished by Na ion deposition.

VI. ANALYSIS AND DISCUSSION OF THE RESULTS

The findings that have been discussed up to now are supported by an analysis of the electronic structure. It is known that the interaction between the magnetic layers is mediated by the confined delocalized electrons in Cu layers [23,59], which is a direct consequence of the spin-polarized potential at the Fe/Cu interfaces. Indeed, it is observed that the net charge carriers for negative (positive) charge doping spill (deplete) mainly at the surface, and minimum variation exists below the surface. At this stage, there are two factors that can impose changes on the potential of the quantum-well-like structure. The first one is related to changes in the boundary conditions as a result of the relative alignment of the two magnetic layers, parallel or antiparallel. Secondly, the addition or removal of extra charge can alter the Fe/Cu

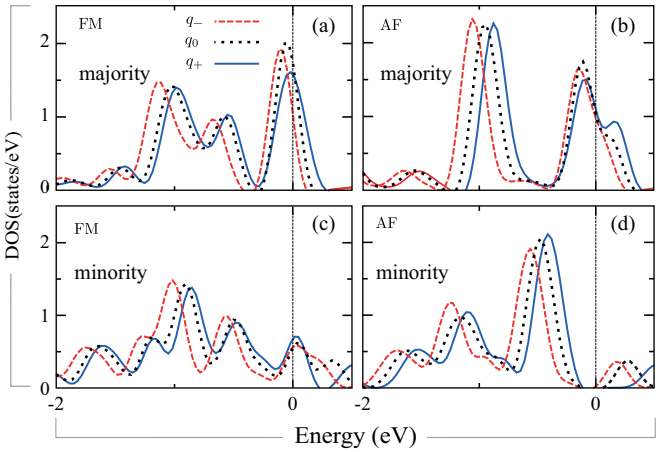

FIG. 5. (Color online) The spin-polarized quantum-well states of all Cu spacer layers for FM [(a) and (c)] and AF [(b) and (d)] orders, at different charge states of the supercell. The majority and minority DOS are presented on the upper [(a) and (b)] and lower [(c) and (d)] panel, respectively. The densities of states are plotted for positive ($q_+ = 1h$, blue full line), negative ($q_- = 1\bar{e}$, red dashed line), and neutral (dotted line) $Fe/Cu_4/Fe$ multilayers. The DOSs are plotted using $4 \times 5k$ points, close to the center of Brillouin zone, within the radius of 0.04 $Å^{-1}$. The vertical dashed line at zero-energy level represents the Fermi energy.

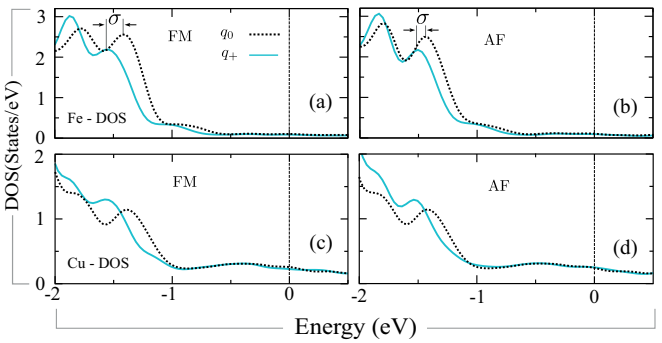

FIG. 6. (Color online) The majority electron density of states (for d orbitals) of the top Fe layer $Fe/Cu_4/Fe$ for both FM (a) and AF (b) configurations. The shift in the DOS (σ) is compared for the neutral system and when it is charged with 1.0 h per unit cell. The majority density of states for the Cu layer interfaced with the top Fe layer is shown in the lower panel. The Cu-DOS is plotted for the cases in which the $Fe/Cu_4/Fe$ trilayer is coupled ferromagnetically (c) and antiferromagnetically (b). The densities of states are integrated over the whole Brillouin zone. The vertical dashed line at the zero-energy level represents the Fermi energy.

interface as well as the reflectivity of the confined states at the boundaries [23]. These two modifications will affect the nature of the confinement, as they result in an additional scattering constraint of the quantum-well states. In Fig. 5, the effect of these two parameters on the spin-polarized QWSs of the $Fe/Cu_4/Fe$ trilayer is depicted. In this figure, the $s + p$ density of states of the coupling medium, for all Cu layers, is plotted for FM (a) and AF (b) coupling. We have considered three charge states, namely positive (q_+), neutral (q_o), and negative (q_-). An electron or hole doping of the order of 1 $\bar{e}$ (h) is used for the charged systems. One can deduce that the shift of the spin-polarized QWS in the energy scale depends on the polarization of the charge doping, and consequently this can alter the nature of the magnetic coupling. For both magnetic orders, the positive (negative) charge doping shifts the QWS toward higher (lower) energies. On the other hand, the variation of the magnetic order between the magnetic layers can be directly inferred from the change in the integrated density of state (DOS), which contributes significantly to the total energy [23,54], $E = \int^{\varepsilon_F} n(\varepsilon)(\varepsilon - \varepsilon_F)d\varepsilon$, where $n(\varepsilon)$ is the density of states. Thus, the change in the IEC is explained from the shift in the DOS of the magnetic layer or the coupling medium for FM and AF configuration at different charge states. As shown in Fig. 5, the shift of the QWS induced by positive charging is more enhanced for AF coupling. The dependence of such a band shift on the magnetic order can lead to stable ferromagnetic coupling in $Fe/Cu_4/Fe$ for positive charging, as is found in Sec. III. It should be noted that the QWSs are calculated by sampling the k points near the center of the Brillouin zone.

To get additional information, the total density of states is also analyzed. More importantly, studying the variation of the electronic structure of the top FeCu interface can also provide more insight into the change of the IEC caused by surface charging. First, we would like to focus on the electronic structure of the magnetic layer in order to elucidate the magnetic reversal scenario once more. For both magnetic orders, the shift of the minority bands caused by the surface charging process shows a minimum difference and is omitted. Unlike for the case of Cu-QWSs (Fig. 5), the majority and minority bands of the Fe layer show opposite shift relative to the neutral system. This leads to an increase or decrease in the exchange splitting as well as the magnetic moment. As shown Figs. 6(a) and 6(b), the majority QWS of the Cu spacer is shifted to higher energy as the $Fe/Cu_4/Fe$ trilayer is positively charged, but the majority DOS of Fe is shifted to lower energies. This is caused by the net charge accumulated/depleted, and the reflectivity of the confined electrons within the quantum-well-like structure (Fe-Cu-Fe) can be modified as well.

In Figs. 6(a) and 6(b), the majority DOS for d orbitals of the top Fe layer, for parallel and antiparallel alignment, at two different charge states is presented. Similarly, the density of states of the Cu atoms that are interfaced with the Fe layer is plotted in Figs. 6(c) and 6(d). From this density of states one can infer that there is a hybridization between the sp states of Cu with d orbitals of Fe. In other words, injecting a positive charge of 1 h per unit cell induces a strong shift (σ) of the majority d bands of Fe toward lower energies by $\sigma = 140$ and 65 meV for FM and AF configurations, respectively. This implies that the majority bands of Fe, in the case of ferromagnetic coupling, are more sensitive to positive charge doping, which leads to a lower total energy and stable ferromagnetic coupling. The reason for such a change of the majority bands is related to the sp-d hybridization of the Cu layer with the top Fe layer. When the system is either negatively or positively charged, the sp states are affected substantially, and this leads to a change in the sp-d hybridization. Evidently, the corresponding shift of the DOS of Cu induced by positive

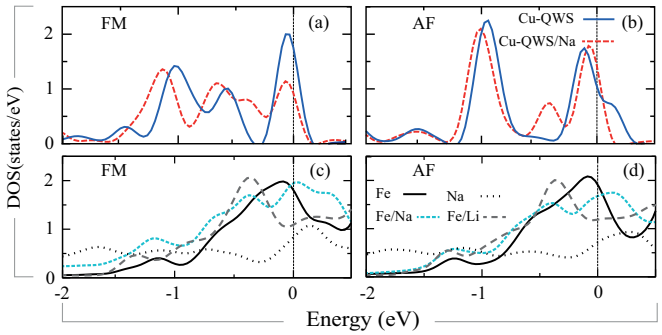

FIG. 7. (Color online) The effect of the Na capping layer in the confined states of the quantum-well-like structure, $Fe/Cu_4/Fe$ (neutral), for FM (a) and AF (b) couplings. The DOSs of the QWS are presented for minority states with Na doping (dashed line) and without Na doping (full line). In the lower panel, the minority electronic density of states (d orbitals) of the top Fe layer is plotted within the FM (c) and AF (d) configurations. In these plots, the DOS clean Fe surface and alkali-metal (Na, Li) -doped Fe surface are represented with full and dashed lines, respectively. The dashed gray line (wider spacing) shows the minority bands of the top Fe in an $Fe/Cu_4/Fe/Li$-$p(1 \times 1)$ multilayer. The DOS for the Na layer is also shown by dotted lines, and it is multiplied by factor of 10. The shift of the majority DOS as a result of Na ion doping is relatively similar, for both FM and AF order, and it is not included. The vertical dashed line at zero-energy level represents the Fermi energy.

charge doping to lower energies has a similar tendency to that of the majority bands of Fe; see Figs. 6(c) and 6(d).

Similar to the case of direct surface charging, some insights into the variations of the magnetic order (by alkali-metal doping) can be inferred by comparing the QWS and the integrated density of states. However, the mechanism by which the IEC is changed via Na or Li doping involves both chemical and electronic effects, unlike that of direct surface charging. In Fig. 7, the minority quantum-well states within the coupling medium of $Fe/Cu_4/Fe$ are presented for FM (a) and AF (b) coupling. In this figure, it is shown that the QWSs, for both FM and AF couplings, are shifted to lower energy as a result of Na doping. Additionally, in Fig. 7 the minority DOS of the top Fe layer in the $Fe/Cu_4/Fe$ trilayer (uncharged) is also shown for both FM (c) and AF (d) couplings as well as the DOS of Na capping layers. Similar to the case of Cu-QWS (upper panel) and Fe-DOS (lower panel), the minority bands are correspondingly shifted to lower energy as a result of the Na capping layer. Clearly, the effect is more pronounced for the case of FM coupling compared with the AF coupling case. Following Na adsorption, more states are displaced to lower energies in the case of FM coupling, leading to stable FM order. Indeed, similar changes are also observed for the bottom magnetic layer, which is mediated by quantum-well states. In Sec. IV, we have seen that reducing the percentage coverage of either Na [Na-$c(2 \times 2)$] or Li-$p(1 \times 1)$ can reverse the magnetic order of $Fe/Cu_4/Fe$ from AF order to FM order. To get some insight about these differences, we have added the minority-DOS plot for the top Fe layer [gray dashed line, Figs. 7(c) and 7(d)] when the $Fe/Cu_4/Fe$ is doped with Li-$p(1 \times 1)$. It seems that Li does not bring about a strong change to the spin-polarized electronic structure of the Fe layer, which can induce magnetic reversal. According to Figs. 7(c) and 7(d), the shift of the minority bands of Fe to lower energies by the Li-$p(1 \times 1)$ overlayer, for FM and AF couplings, is not as pronounced as in the case of Na-$p(1 \times 1)$ doping. On the contrary, the more minority DOS of Fe layers shifts to lower energy for the case of AF coupling, which can only change the value of the exchange coupling.

We have discussed the impact of varying the surface electronic structure with surface charging or alkali-metal doping. Now, it is important to compare the effects of both surface charging techniques on the IEC. From Figs. 1 and 2 one can see that covering the magnetic layers with Na-$c(1 \times 1)$ does not necessarily lead to a change similar to that of electron doping (1 $\bar{e}$/unit cell). As an example, for the $Fe/Cu_4/Fe$ trilayer, electron doping and Na [Na-$c(1 \times 1)$] deposition have opposite effects relative to the neutral system. However, the impact of the submonolayer Na-$c(2 \times 2)$ and direct surface charging techniques consistently favor the same magnetic orders for almost all Cu spacer thicknesses.

Using atomistic spin-model simulations, we revealed a magnetic hardening mechanism in FePt multilayers by Na ion doping. These variations in the MAE are mainly caused by a combined effect of the interlayer exchange coupling and the changes in surface electronic structure induced by Na. To elucidate the first case, we compared the MAE for three different cases, i.e., Fe/Pt_5, $Fe/Pt_5/Fe$, and $Fe/Pt_5/Fe/Na$ on Pt(001). The MAE of the first structure is found to be 1.6 meV. When the bilayer Fe/Pt_5 is terminated with the Fe layer ($Fe/Pt_5/Fe$), it leads to the onset of the effect of interlayer exchange coupling on magnetic anisotropy. The added (top) magnetic layer, which couples ferromagnetically with the bottom Fe layer, brings about a small change to the MAE. However, deposition of the Na ion increases the MAE enormously. Here the strong change in the MAE is a ramification of the IEC and the change in the electronic structure of the FePt interfaces. This implies that both the magnetic order and the interface electronic structure are relevant parameters that could affect the MAE by varying the spin-orbit coupling. In other words, the contribution of the spin-orbit coupling to each axis of magnetization, in-plane or out-of plane, determines the MAE. For instance, in FePt multilayers the coupling between occupied and unoccupied states of d_δ and d_π orbitals is identified as dominant among the minority d orbitals [47,60], where $d_\delta = d_{x^2-y^2} + d_{xy}$ and $d_\pi = d_{xz(yz)} + d_{z^2}$. For the case of $Fe/Pt_5/Fe/Na$, the orbitals d_δ (d_π) are less (more) degenerate near the Fermi energy for the top Fe layer as compared to the lower ones. This tends to lower the energy when the magnetization of the multilayer is perpendicular to the surface, leading to a substantial increase in the MAE for the bottom FePt interfaces. In addition, the magnetic moment as well as the induced magnetic moment for the lower FePt interfaces have increased as a result of Na capping, and conversely decreased for the top layers.

On the other hand, some of the FePt multilayers with high MAE have stable antiferromagnetic coupling, implying that these FePt thin films could be essential candidates for AF domains [61]. In addition, AF domains have a highly minimized dipolar magnetic interaction between the neighboring bits, and they could play a crucial role in reducing the density of the current magnetic storage device [49]. Additionally, such

AF multilayers can be an integral part of an exchange biased system, and they could have a significant impact on the quest for ultrafast magnetic switching [55,56]. In fact, the switching procedure of relative magnetization by incorporating alkali-metal doping can also be perceived as follows. Regardless of the original magnetic order in the FM/NM/FM trilayer, first one has to overcome the energy barrier (MAE) of the top ferromagnet in order to switch to the opposite direction. The magnetic anisotropy of each magnetic layer in the FePt multilayer was estimated in an earlier section. This energy barrier can certainly be altered by introducing alkali metal into the system, which varies the interface electronic structure. The charge rearrangements are then transformed to magnetic anisotropy through spin-orbit coupling, which results in changes of the relative orientation of the atomic moments. However, these surface charging techniques do not always lead to magnetization reversal. Instead, favorable conditions will be created for other means of spin manipulation mechanisms, e.g., spin-transfer torque [7,8] or electrostatic gating [37,62,63], leading to a switching mechanism assisted by alkali-metal doping. Therefore, once the energy barrier is completely overcome, the system probably settles down to the reversed state.

VII. CONCLUSION

In summary, we have presented a comprehensive study that reveals the effect of two surface-interface charging techniques on the IEC of magnetic layers across Cu and Pt spacers as well as their MAE. Explicitly, in some cases the mutual magnetic orders of fully metallic FM/NM/FM-like structure can be remarkably tuned between ferromagnetic and antiferromagnetic states by the addition or removal of extra charge. Moreover, by employing alkali metals as dopants, we have shown a natural way of space-charge alteration that can reverse the relative magnetic orders in alloyed multilayers and strongly enhance the MAE of Fe/Pt. These effects lead us to the conclusion that alkali-metal-induced charging magnetic surfaces can assist the process of magnetization reversal and can also help to control the spin states as well as the spin dynamics. All in all, our findings suggest that involving alkali metals in the field of spintronics could have a significant impact on efforts to design new functional spintronic devices or quantum computing.

ACKNOWLEDGMENTS

T.R.D. would like to acknowledge Richard F. L. Evans at the University of York for the helpful discussion related to the atomistic model approach. We would also like to thank O. O. Brovko and P. Ruiz-Díaz for the fruitful discussion. This work is supported by the Deutsche Forschungsgemeinschaft (DFG) within the SFB 762 and project "Structure and magnetism of cluster ensembles on metal surfaces: Microscopic theory of the fundamental interactions."

[1] E. Y. Tsymbal, Electric toggling of magnets, Nat. Mater. **11**, 12 (2012).
[2] N. A. Spaldin, and M. Feibig, The renaissance of magnetoelectric multiferroics, Science **309**, 391 (2005).
[3] F. S. G. Binasch, P. Grunberg, and W. Zinn, Enhanced magnetoresistance in layered magnetic structures, Phys. Rev. B **39**, 4828 (1989).
[4] M. N. Baibich, J. M. Broto, A. Fert, F. Nguyen, Van Dau, F. Petroff, P. Eitenne, G. Creuzet, A. Friederich, and J. Chazelas, Giant magnetoresistance of (001)Fe/(001)Cr magnetic superlattices, Phys. Rev. Lett. **61**, 2472 (1988).
[5] S. S. P. Parkin, C. Kaiser, A. Panchula, P. M. Rice, B. Huges, M. Samant, and S.-H. Yang, Giant tunneling magnetoresistance at room temperature with MgO. (100) tunnel barriers, Nat. Mater. **3**, 862 (2004).
[6] M. Kryder, and C. S. Kim, After hard drives what comes next?, IEEE Trans. Magn. **45**, 3406 (2009).
[7] J. Slonczewski, Current-driven excitation of magnetic multilayers, J. Magn. Magn. Mater. **159**, L1 (1996).
[8] L. Berger, Emission of spin waves by magnetic multilayer traversed by a current, Phys. Rev. B **54**, 9353 (1996).
[9] W. G. Wang and C. L. Chien, Voltage-induced switching in magnetic tunnel junctions with perpendicular magnetic anisotropy, J. Phys. D **46**, 074004 (2013).
[10] J. Zhu, J. A. Katine, G. E. Rowlands, Y.-J. Chen, Z. Duan, J. G. Alzate, P. Upadhyaya, J. Langer, P. K. Amiri, K. L. Wang, and I. N. Krivorotov, Voltage-induced ferromagnetic resonance in magnetic tunnel junctions, Phys. Rev. Lett. **108**, 197203 (2012).
[11] H.-C. Wu, O. N. Mryasov, M. Abid, K. Radican, and I. V. Shvets, Magnetization states of all-oxide spin valves controlled by charge-orbital ordering of coupled ferromagnets, Sci. Rep. **3**, 1830 (2013).
[12] K. Nakamura, R. Shimabukuro, Y. Fujiwara, T. Akiyama, T. Ito, and A. J. Freeman, Giant modification of the magnetocrystalline anisotropy in transition-metal monolayers by an external electric field, Phys. Rev. Lett. **102**, 187201 (2009).
[13] O. O. Brovko, P. Ruiz-Díaz, T. R. Dasa, and V. S. Stepanyuk, Controlling magnetism on metal surfaces with non-magnetic means: Electric fields and surface charging, J. Phys.: Condens. Matter **26**, 093001 (2014).
[14] M. Tsujikawa and T. Oda, Finite electric field effects in the large perpendicular magnetic anisotropy surface Pt/Fe/Pt(001): A first-principles study, Phys. Rev. Lett. **102**, 247203 (2009).
[15] P. Ruiz-Díaz, T. R. Dasa, and V. S. Stepanyuk, Tuning magnetic anisotropy in metallic multilayers by surface charging: An *ab-initio* study, Phys. Rev. Lett. **110**, 267203 (2013).
[16] S. Subkow and M. Fähnle, Electron theory of magnetoelectric effects in metallic ferromagnetic nanostructures, Phys. Rev. B **84**, 054443 (2011).
[17] S. Sahoo, S. Polisetty, C.-G. Duan, S. Jaswal, E. Tsymbal, and C. Binek, Ferroelectric control of magnetism in $BaTiO_3$Fe heterostructures via interface strain coupling, Phys. Rev. B **76**, 092108 (2007).
[18] A. Sonntag, J. Hermenau, A. Schlenhoff, J. Friedlein, S. Krause, and R. Wiesendanger, Electric-field-induced magnetic

anisotropy in a nanomagnet investigated on the atomic scale, Phys. Rev. Lett. **112**, 017204 (2014).

[19] C. Bi, Y. Liu, T. Newhouse-Illige, M. Xu, M. Rosales, J. W. Freeland, O. Mryasov, S. Zhang, S. G. E. te Velthuis, and W. G. Wang, Reversible control of Co magnetism by voltage-induced oxidation, Phys. Rev. Lett. **113**, 267202 (2014).

[20] N. A. Pertsev and H. Kohlstedt, Resistive switching via the converse magnetoelectric effect in ferromagnetic multilayers on ferroelectric substrates, Nanotechnology **21**, 475202 (2010).

[21] J. T. Heron, M. Trassin, K. Ashraf, M. Gajek, Q. He, S. Y. Yang, D. E. Nikonov, Y-H. Chu, S. Salahuddin, and R. Ramesh, Electric-field-induced magnetization reversal in a ferromagnet-multiferroic heterostructure, Phys. Rev. Lett. **107**, 217202 (2011).

[22] M. Fechner, P. Zahn, S. Ostanin, M. Bibes, and I. Mertig, Switching magnetization by 180 with an electric field, Phys. Rev. Lett. **108**, 197206 (2012).

[23] P. Bruno, and C. Chappert, Ruderman-Kittel theory of oscillatory interlayer exchange coupling, Phys. Rev. B **46**, 261 (1992).

[24] W.-S. Zhang, B.-Z. Li, and Y. Li, Conductance, magnetoresistance, and interlayer exchange coupling in magnetic tunnel junctions with nonmagnetic metallic spacers and finite thick ferromagnetic layers, Phys. Rev. B **58**, 14959 (1998).

[25] G. Kresse and D. Joubert, From ultrasoft pseudopotentials to the projector augmented-wave method, Phys. Rev. B **59**, 1758 (1999).

[26] G. Kresse and J. Hafner, Ab initio molecular dynamics for liquid metals, Phys. Rev. B **47**, 558 (1993).

[27] G. Kresse and J. Furthmüller, Efficient iterative schemes for ab initio total-energy calculations using a plane-wave basis set, Phys. Rev. B **54**, 11169 (1996).

[28] D. M. Ceperley and B. J. Alder, Ground state of the electron gas by a stochastic method, Phys. Rev. Lett. **45**, 566 (1980).

[29] The layers in the slabs are initially interspaced with a bulk interlayer distance of 1.95 Å, associated with the calculated lattice constant of fcc Pt (3.91 Å). Later on, the geometry of the system is relaxed until the force on each atom is less than 5 meV/Å. The Fe/Cu(Pt)/Fe layers are supported by a substrate that consists of ten Pt layers.

[30] G. Makov and M. C. Payne, Periodic boundary conditions in ab initio calculations, Phys. Rev. B **51**, 4014 (1995).

[31] G. Kresse and O. Lebacq, VASP Manual, http://cms.mpi.univie.ac.at/vasp/vasp/.

[32] R. F. L. Evans, W. J. Fan, P. Chureemart, T. A. Ostler, M. O. A. Ellis, and R. W. Chantrell, Atomistic spin model simulations of magnetic nanomaterials, J. Phys.: Condens. Matter **26**, 103202 (2014); http://vampire.york.ac.uk/.

[33] W. F. Brown, Thermal fluctuations of a single-domain particle, Phys. Rev. **130**, 1677 (1963).

[34] Electron charge is represented with "$\bar{e}$," whereas "h" depicts a hole charge, being $-e$. Similarly, arbitrary positive and negative charge concentrations within the multilayers are depicted with q_+ and q_- signs, respectively. The parameters that are employed to calculate the MAE and IEC are tested for their reliability. For instance, for $Fe/Pt_3/Fe$, increasing the number of k-points to $25 \times 25 \times 1$ (where cutoff energy $= 430$ eV), the MAE varies only by 6%, relative to the one reported in the paper. Additionally, when the k-points and plane-wave cutoff energy are $21 \times 21 \times 1$ and 500 eV, respectively, the MAE changes only by 3%. The conclusions are not affected by these variations.

[35] M. Weisheit, S. Fähler, A. Marty, Y. Souche, C. Poinsignon, and D. Givord, Electric field-induced modification of magnetism in thin-film ferromagnets, Science **315**, 349 (2007).

[36] H. Zhang, M. Richter, K. Koepernik, I. Opahle, F. Tasnádi, and H. Eschrig, Electric-field control of surface magnetic anisotropy: A density functional approach, New J. Phys. **11**, 043007 (2009).

[37] T. Maruyama, Y. Shiota, T. Nozaki, K. Ohta, N. Toda, M. Mizuguchi, A. A. Tulapurkar, T. Shinjo, M. Shiraishi, S. Mizukami, Y. Ando, and Y. Suzuki, Large voltage-induced magnetic anisotropy change in a few atomic layers of iron, Nature Nanotech. **4**, 158 (2009).

[38] C. Krull, R. Robles, A. Mugarza, and P. Gambardella, Site- and orbital-dependent charge donation and spin manipulation in electron-doped metal phthalocyanines, Nat. Mater. **12**, 337 (2013).

[39] J. Repp, G. Meyer, F. E. Olsson, and M. Persson, Controlling the charge state of individual gold adatoms, Science **305**, 493 (2004).

[40] G. Fratesi, Potential energy surface of alkali atoms adsorbed on Cu(001), Phys. Rev. B **80**, 045422 (2009).

[41] A. N. Rudenko, F. J. Keil, M. I. Katsnelson, and A. I. Lichtenstein, Exchange interactions and frustrated magnetism in single-side hydrogenated and fluorinated graphene, Phys. Rev. B **88**, 081405(R) (2013).

[42] M. Cinchetti, S. Neuschwander, A. Fischer, A. Ruffing, S. Mathias, J.-P. Wüstenberg, and M. Aeschlimann, Tailoring the spin functionality of a hybrid metal-organic interface by means of alkali-metal doping, Phys. Rev. Lett. **104**, 217602 (2010).

[43] J. Zhao, N. Pontius, A. Winkelmann, V. Sametoglu, A. Kubo, A. G. Borisov, D. Snchez-Portal, V. M. Silkin, E. V. Chulkov, P. M. Echenique, and H. Petek, Electronic potential of a chemisorption interface, Phys. Rev. B **78**, 085419 (2008).

[44] J. Mathon, M. Villeret, A. Umerski, R. B. Muniz, J. d' Albuquerque e Castro, and D. M. Edwards, Quantum-well theory of the exchange coupling in magnetic multilayers with application to Co/Cu/Co(001), Phys. Rev. B **56**, 11797 (1997).

[45] M. Kowalewski, B. Heinrich, T. C. Schulthess, and W. H. Butler, First principles calculations of interlayer exchange coupling in bcc Fe/Cu/Fe structures, IEEE Trans. Magn. **34**, 1225 (1998).

[46] Y. Yamauchi, M. Kurahashi, T. Suzuki, and X. Ju, Influence of submonolayers of sodium on the spin polarization of iron outmost surfaces, J. Appl. Phys. **93**, 8734 (2003).

[47] T. R. Dasa, P. Ruiz-Díaz, O. O. Brovko, and V. S. Stepanyuk, Tailoring magnetic properties of metallic thin films with quantum well states and external electric fields, Phys. Rev. B **88**, 104409 (2013).

[48] J. B. Staunton, S. Ostanin, S. S. A. Razee, B. L. Gyorffy, L. Szunyogh, B. Ginatempo, and E. Bruno, Temperature dependent magnetic anisotropy in metallic magnets from an ab initio electronic structure theory: $L1_0$-ordered FePt, Phys. Rev. Lett. **93**, 257204 (2004).

[49] T. Klemmer, N. Shukla, C. Liu, X. Wu, E. Svedberg, O. Mryasov, R. Chantrell, D. Weller, M. Tanase, and D. Laughlin, Structural studies of L10 FePt nanoparticles, Appl. Phys. Lett. **81**, 2220 (2002).

[50] L. V. Dzemiantsova, M. Hortamani, C. Hanneken, A. Kubetzka, K. von Bergmann, and R. Wiesendanger, Magnetic coupling

of single Co adatoms to a Co underlayer of variable thickness, Phys. Rev. B **86**, 094427 (2012).

[51] F. Yildiz, M. Przybylski, and J. Kirschner, Direct evidence of a nonorthogonal magnetization configuration in single crystalline system, Phys. Rev. Lett. **103**, 147203 (2009).

[52] S. Blizak, G. Bihlmayer, S. Blügel, and S. E. H. Abaidia, Interlayer exchange coupling between FeCo and Co ultrathin films through Rh(001) spacers, Phys. Rev. B **91**, 014408 (2015).

[53] P. J. H. Bloemen, M. T. Johnson, M. T. H. van de Vorst, R. Coehoorn, J. J. de Vries, R. Jungblut, J. aan de Stegge, A. Reinders, and W. J. M. de Jonge, Magnetic layer thickness dependence of the interlayer exchange coupling in (001) Co/Cu/Co, Phys. Rev. Lett. **72**, 764 (1994).

[54] P. Lang, L. Nordström, K. Wildberger, R. Zeller, P. H. Dederichs, and T. Hoshino, Ab initio calculations of interaction energies of magnetic layers in noble metals: Co/Cu(100), Phys. Rev. B **53**, 9092 (1996).

[55] I. Radu, K. Vahaplar, C. Stamm, T. Kachel, N. Pontius, H. A. Dürr, T. A. Ostler, J. Barker, R. F. L. Evans, R. W. Chantrell, A. Tsukamoto, A. Itoh, A. Kirilyuk, Th. Rasing, and A. V. Kimel, Transient ferromagnetic-like state mediating ultrafast reversal of antiferromagnetically coupled spins, Nature (London) **472**, 205 (2011).

[56] A. V. Kimel, A. Kirilyuk, A. Tsvetkov, R. V. Pisarev, and Th. Rasing, Laser-induced ultrafast spin reorientation in the antiferromagnet $TmFeO_3$, Nature (London) **429**, 850 (2004).

[57] U. Nowak, in *Annual Reviews of Computational Physics IX* (World Scientific, Singapore, 2001), p. 105.

[58] Independent calculations are done in order to find the exchange parameters J_1, J_2, and J_3 from the supercells Pt(001)/Fe/(Na), Pt(001)/Fe/Pt_5, and Pt(001)/Fe/Pt_5/Fe/(Na), respectively. Based on the number of nearest neighbors (N_n) and the magnetic moments (m_i,m_j) of the interacting spins, the parameters are determined according to $E_{\mathrm{AF}} - E_{\mathrm{FM}} = 2N_n J_{ij} m_i m_j$. Regarding the magnetic anisotropy, first we calculate MAE of Pt(001)/Fe/Pt_5 and Pt(001)/Fe/Pt_5/Fe/Na multilayers, separately. Then we took the difference in the MAE of these multilayers, the changes in the spin and orbital moments, and analysis on the DOS (based on second-order perturbation theory [60]) in order to estimate of the MAE of each magnetic layer.

[59] O. Brovko, P. Ignatiev, V. Stepanyuk, and P. Bruno, Tailoring exchange interactions in engineered nanostructures: An ab initio study, Phys. Rev. Lett. **101**, 036809 (2008).

[60] D. S. Wang, R. Wu, and A. J. Freeman, First-principles theory of surface magnetocrystalline anisotropy and the diatomic-pair model, Phys. Rev. B **47**, 14932 (1993).

[61] F Nolting, A. Scholl, J. Stöhr, J. W. Seo, J. Fompeyrine, H. Siegwart, J.-P. Locquet, S. Anders, J. Lüning, E. E. Fullerton, M. F. Toney, M. R. Scheinfein, and H. A. Padmore, Direct observation of the alignment of ferromagnetic spins by antiferromagnetic spins, Nature (London) **405**, 767 (2000).

[62] U. Bauer, M. Przybylski, and G. S. D. Beach, Voltage control of magnetic anisotropy in Fe films with quantum well states, Phys. Rev. B **89**, 174402 (2014).

[63] K. Shimamura, D. Chiba, S. Ono, S. Fukami, N. Ishiwata, M. Kawaguchi, K. Kobayashi, and T. Ono, Electrical control of Curie temperature in cobalt using an ionic liquid film, Appl. Phys. Lett. **100**, 122402 (2012).